Nitro-polycyclic aromatic hydrocarbons - gas-particle partitioning, mass size distribution, and formation along transport in marine and continental background air

Gerhard Lammel [1,2*], Marie D. Mulder [1], Pourya Shahpoury [2], Petr Kukučka [1], Hana Lišková [1], Petra Přibylová [1], Roman Prokeš [1], Gerhard Wotawa [3]

[1] Masaryk University, Research Centre for Toxic Compounds in the Environment, Brno, Czech Republic

[2] Max Planck Institute for Chemistry, Multiphase Chemistry Department, Mainz, Germany

[3] Zentralanstalt fuer Meteorologie und Geodynamik, Wien, Austria

*lammel@recetox.muni.cz

Abstract

Nitro-polycyclic aromatic hydrocarbons (NPAH) are ubiquitous in polluted air but little is known about their abundance in background air. NPAHs were studied at one marine and one continental background site i.e., a coastal site in the southern Aegean Sea (summer 2012) and a site in the central Great Hungarian Plain (summer 2013), together with the parent compounds, PAHs. A Lagrangian particle dispersion model was used to track air mass history. Based on Lagrangian particle statistics, the urban influence on samples was quantified for the first time as a fractional dose to which the collected volume of air had been exposed to.

At the remote marine site, the 3-4 ring NPAH (sum of 11 targeted species) concentration was 23.7 pg m^{-3} while the concentration of 4-ring PAHs (6 species) was 426 pg m^{-3}. 2-nitrofluoranthene (2NFLT) and 3-nitrophenanthrene were the most abundant NPAHs. Urban fractional doses in the range <0.002–5.4% were calculated. At the continental site, the Σ_{11} 3-4rNPAH and Σ_6 4rPAH were 58 and 663 pg m^{-3}, respectively, with 9-nitroanthracene and 2NFLT being highest concentrated amongst the targeted NPAHs. The NPAH levels observed in the marine background are the lowest ever reported and remarkably lower, by more than one order of magnitude, than one decade before. Day-night variation of NPAHs at the

continental site reflected shorter lifetime during the day, possibly because of photolysis of some NPAHs. The yields of formation of 2NFLT and 2-nitropyrene (2NPYR) in marine air seem to be close to the yields for OH-initiated photochemistry observed in laboratory experiments under high NO_x conditions. Good agreement is found for prediction of NPAH gas-particle partitioning using a multi-phase poly-parameter linear free energy relationship. Sorption to soot is found less significant for gas-particle partitioning of NPAHs than for PAHs. The NPAH levels determined in the southeastern outflow of Europe confirm intercontinental transport potential.

Keywords: long-range transport potential, semi-volatile organic compounds, PAH photochemistry,

1. Introduction

PAHs may undergo chemical transformations in the gaseous and in the particulate phase (Finlayson-Pitts and Pitts, 2000; Keyte et al., 2013). Nitro-PAHs (NPAHs) observed in urban and rural areas (Nielsen et al., 1984; Feilberg et al., 2001; Finlayson-Pitts and Pitts, 2000; Keyte et al., 2013) and predicted based on smog-chamber experiments (Atkinson and Arey, 1994), seem to be most significant derivatives: Mutagenicity of atmospheric aerosols in general is mostly related to NPAHs (Grosjean et al., 1983; Garner et al., 1986; Finlayson-Pitts and Pitts, 2000; Claxton et al., 2004; Hayakawa, 2016). A large part, more than one third, of the mutagen potential of ambient aerosols may be attributable to NPAHs (Schuetzle, 1983).

Secondary formation of NPAH from PAHs is thought to occur on short time scales (hours). This has been observed for PAHs collected on filters (Ringuet et al., 2012a; Zimmermann et al., 2013; Jaryasopit et al., 2014a, 2014b), and also in in urban plumes (Bamford and Baker, 2003; Arey et al., 1989; Reisen and Arey, 2005). Although many NPAHs are emitted from road traffic, only a few are abundant in this source type (Arey, 1998; Keyte et al., 2013 and 2016; Inomata et al., 2015; Alves et al., 2016). The occurrence of various isomers of nitrofluoranthene (NFLT) and nitropyrene (NPYR) can be used to study PAH sources, PAH chemical transformations and the role of the photo-oxidants hydroxyl radical (OH) and nitrate radical (NO_3) (Ciccioli et al., 1996; Finlayson-Pitts and Pitts 2000). E.g., 3- and 2-nitrofluoranthene (3-, 2NFLT) are indicative of primary and secondary sources, respectively. These substances have been suggested as tracers for air pollution on the time scales of hours

to days (Ciccioli et al., 1996; Finlayson-Pitts and Pitts 2000; Keyte et al. 2013), but their atmospheric lifetimes are still unknown.

Like their precursors, NPAHs are semivolatile organic compounds (SVOCs), partitioning between the phases of the atmospheric aerosol. Similar to other SVOCs, the NPAHs' phase distribution was found to depend on temperature (summer and winter campaigns in the Alps; Albinet et al., 2008b) and results from both absorptive as well as adsorptive contributions (Tomaz et al., 2016). NPAHs have primarily been observed in polluted areas (e.g. Pitts et al., 1985; Ramdahl et al., 1986; Garner et al., 1986; Albinet et al., 2007 and 2008a; Ringuet et al., 2012a and 2012b; Zimmermann et al., 2012; Barrado et al., 2013; Li et al., 2016). Though there are a few studies in rural environments i.e., in Germany (Ciccioli et al., 1996), in the French Alps (100-1000 pg m^{-3} range for the sum of 10 NPAHs; Albinet et al., 2008a) and in northern China (Li et al., 2016). Very few measurements have been performed in the remote atmospheric environment i.e., in the Mediterranean (Tsapakis and Stephanou, 2007), high altitude sites in the Himalayas (single data; Ciccioli et al. 1996) and French Alps (Albinet et al., 2008a), and in the Arctic (with so-called Arctic haze; Masclet et al. 1988; Halsall et al. 2001). With regard to the long-range transport potential, the state of the knowledge is that at least some NPAHs are expected to go into intercontinental transport (Lafontaine et al., 2015) and might be ubiquitous in the global atmosphere (Ciccioli et al., 1996).

However, there is limited NPAH data from remote atmospheric environments is obvious and little is known about their long-range transport potential. The aim of this study was to characterise the long-range transport potential of NPAHs by measurements at remote sites of Europe, addressing the continental background and the outflow of the continent.

2. Methodology

2.1 Sampling

High-volume air sampling was conducted at a marine background site, Finokalia (35.3°N/25.7°E, 250 m a.s.l.), in the context of a coordinated field experiment 2-13 July 2012 (Lammel et al., 2015) and at a continental background site in central Europe, K-puszta (46º58'N/19º33'E, 125 m a.s.l.; Degrendele et al., 2016), 5-16 August 2013. The Finokalia site is located on a cliff at the northern coast of Crete, some 70 km east of major significant anthropogenic emissions (Iraklion, a city of 100000 inhabitants with airport and industries; Mihalopoulos et al., 1997; Kouvarakis et al., 2000). The K-puszta site is located on a clearing, characterised by uncultivated grassland, in a mostly coniferous forest in the Hungarian

(Pannonian) Great Plain, ca. 70 km and 270 km southeast of Budapest and Vienna, respectively (≈2 mn inhabitants each). The background site character of both observatories had been demonstrated (Borbély-Kiss et al., 1988; Kouvarakis et al., 2000; Vrekoussis et al., 2005). Meteorological and trace gas measurements are covered by both observatories, which are stations of the EMEP network (EMEP, 2015).

High volume air samples were collected using a HV-100P (Baghirra, Prague, Czech Republic), equipped with a multi-stage cascade impactor (Andersen Instruments Inc., Fultonville, New York, USA, series 230, model 235) with five impactor stages, corresponding to 10–7.2, 7.2–3, 3–1.5, 1.5–0.95 and 0.95–0.49 μm of aerodynamic particle size, D, (spaced roughly equal ΔlogD), a backup filter collecting particles < 0.49 μm and, downstream, two polyurethane foam plugs (PUFs, Molitan, Břeclav, Czech Republic, density 0.030 g cm^{-3}, placed in a glass cartridge), together 10 cm high. Particles were sampled on slotted QFF substrates (TE-230-QZ, Tisch Environmental Inc., Cleves, USA, 14.3 × 13.7 cm) and glass fibre filters (Whatman, 20.3 × 25.4 cm). The filters had been cleaned prior to use by heating 108 (330°C). PUFs were cleaned (8 hour-extraction in acetone and 8 hours in dichloromethane (DCM)), wrapped in two layers of aluminum foil, placed into zip-lock polyethylene bags and kept in the freezer prior to deployment. The sampler was operated at constant flow rate of 68 m3 h^{-1}. Day/night sampling (changing at sunset and sunrise) of gaseous samples (PUF) was performed at both sites (V = 600-1000 m³), while at the marine site the impactor filter (QFF) samples were collected over 24 h (5) or 48 h (3).

PUFs were cleaned (8 hour-extraction in acetone and 8 hours in dichloromethane (DCM)), wrapped in two layers of aluminum foil, placed into zip-lock polyethylene bags and kept in the freezer prior to deployment. The sampler was operated at constant flow rate of 68 m^3 h^{-1}. Day/night sampling of gaseous samples (PUF) was performed at both sites (12 h, V ≈ 700 m³), while at the marine site the impactor filter (QFF) samples were collected over 12 h (n = 1), 24 h (4) or 48 h (3).

Particle number concentration, N, was determined by an optical particle counter (Grimm model 107, Ainring, 31 channels between 0.25 and 32 mm of aerodynamic particle diameter, D). Aerosol surface concentration, S (cm^{-1}), was derived as $S = \pi \Sigma_i N_i D_i^2$ assuming sphericity. Hereby, true S will be underestimated, in particular if particles of irregular form were abundant (e.g. Jaenicke, 1988). Comparisons with absolute methods (e.g. Pandis, et al. 1991) suggest that the discrepancy may reach up to a factor of 2-3. The mass median diameter

(D_m, µm), was derived as $\log D_m = \Sigma_i m_i \log D_i / \Sigma_i m_i$ with m_i denoting the mass in size class i, D_i being the geometric mean diameter collected on stage i of the cascade impactor.

2.2 Chemical analysis

All air samples were extracted with DCM using an automatic warm Soxhlet extractor (Büchi B-811, Switzerland). Deuterated PAHs (D8-naphthalene, D10-phenanthrene, D12-perylene; Wellington Laboratories, Canada) were used as surrogate standards for both PAHs and NPAHs. Deuterated PAHs proved to be suitable surrogate standards for NPAHs. These were spiked on each PUF prior to extraction. The extract was split in two parts, 1/9 for PAHs and Nitro-PAHs analysis, 9/10 for PBDEs, PCBs and OCPs. The PAHs and Nitro-PAHs aliquot was a subject to open column chromatography clean-up. Glass column (1 cm i.d.) was filled with 5 g activated silica (150°C for 12 h), sample was loaded and eluted with 10 mL *n*-hexane, followed by 40 mL DCM. The cleaned sample was evaporated under a stream of nitrogen in a TurboVap II apparatus (Biotage, Sweden), transferred into a conical GC vial and spiked with recovery standard, terphenyl, the volume was reduced to 100 µL.

GC-MS analysis of 4-ring PAHs (fluoranthene (FLT), pyrene (PYR), benzo(b)fluorene (BBN), benzo(a)anthracene (BAA), triphenylene (TPH) and chrysene (CHR)) and 2-4 ring NPAHs (1- and 2-nitronaphthalin (1-, 2NNAP), 3- and 5-nitroacenaphthene (3-, 5NACE), 2-nitrofluorene (2NFLN), 9-nitroanthracen (9NANT), 3- and 9-nitrophenanthren (3-, 9NPHE), 2- and 3-nitrofluoranthene (2-, 3NFLT), 1- and 2-nitropyrene (1-, 2NPYR), 7-nitrobenz(a)anthracene (7NBAA), 6-nitrochrysene (6NCHR) was performed using a gas chromatograph atmospheric pressure chemical ionization tandem mass spectrometer (GC-APCI-MS/MS) instrument, Agilent 7890A GC (Agilent, USA), equipped with a 60m × 0.25mm × 0.25um DB-5MSUI column (Agilent, J&W, USA), coupled to Waters Xevo TQ-S (Waters, UK). Injection was 1 µL splitless at 280°C, with He as carrier gas at constant flow 1.5 mL min^{-1}. The GC oven temperature program was as follows: 90°C (1 min), 40°C/min to150°C, 5°C/min to 250°C (5 min) and 10°C/min to 320°C (5 min). APCI was used in charge transfer conditions. The isomers 2- and 3NFLT were not separated by the GC method, but co-eluted and are reported as sum.

Recovery of native analytes varied 72-102% for PAHs and deuterated PAHs, 70-110% for NPAHs (details see supplementary material (SM), Table S1a). The results were not recovery corrected. The mean of field blank values was subtracted from the sample values. Values below the mean + 3 standard deviations of the field blank values were considered to be

<LOQ. Field blank values of some analytes in air samples were below the instrument limit of quantification (ILOQ), which corresponded to 0.004-0.069 pg m^{-3} for NPAHs (except for 1NNAP for which it ranged 0.60-0.87 pg m^{-3}) and 0.010-0.126 pg m^{-3} for 4-ring PAHs (except for FLT and PYR for which it ranged 0.17-0.59 pg m^{-3}) (Table S1).

Higher LOQs were determined for some of the NPAHs and for all 4-ring PAHs in gaseous air samples (PUFs), namely 0.006-0.009 ng (corresponding to 3.5-8.0 pg m^{-3}) for 3NACE and 2NPYR, 0.028-0.097 (corresponding to 16-86 pg m^{-3}) for 2NNAP, 2NFLT and 1NPYR, and 0.10-0.27 ng (corresponding to ≈60-240 pg m^{-3}) for 4-ring PAHs (except for FLT and PYR for which it was 1.71 and 1.05 ng, respectively, corresponding to ≈600-1500 pg m^{-3}). In particulate phase samples, where separate field blanks for the 2 different QFFs were determined (on the impactor stages on one hand side and the backup filter on the other hand side), higher LOQs were determined for some of the NPAHs and for all 4-ring PAHs, namely 0.008-0.089 ng (corresponding to 4.6-79 pg m^{-3}) for 2NNAP, 2NFLT, 1NPYR and 2NPYR, 0.26-0.31 ng (corresponding to 150-274 pg m^{-3}) for 9NANT, and 0.05-0.22 ng (corresponding to ≈30-200 pg m^{-3}) for 4-ring PAHs (except for FLT and PYR for which it was 0.79 and 0.36 ng, respectively, corresponding to ≈200-700 pg m^{-3}).

The breakthrough in PUF samples was estimated (Pankow, 1989; ACD, 2015; Melymuk et al., 2016), and as a consequence, 2-3 ring PAHs and 2-ring NPAHs results were excluded from this study as their sampling may have been incomplete. We, therefore, report $\Sigma_6$4rPAH and Σ_{11}3-4rNPAH.

Particulate matter mass (PM_{10}) was determined by gravimetry (microbalance, filters accommodated to stable temperature and humidity, 3 replicate weighings), and organic matter (OM) and elemental carbon (EC) contents of PM by a thermal-optical method (Sunset Lab., USA; EUSAAR protocol).

2.3 Gas-particle partitioning

Gas-particle partitioning was studied by applying a multiphase ppLFER model, which was recently introduced (Shahpoury et al., 2016). In brief, partitioning of semivolatile compounds in air can be described (Yamasaki et al., 1982), by

(1) $K_p = c_{ip} / (c_{ig} \times c_{PM})$

where K_p (m^3air (g PM)$^{-1}$) is the temperature dependent partitioning coefficient, c_{PM} (g m^{-3}) is the concentration of particulate matter in air, c_{ip} and c_{ig} are the analyte (i) concentrations (ng m^{-3}) in the particulate and gas phase, respectively. K_p can be predicted using models based on single- and poly-parameter linear free energy relationships (spLFER, ppLFER). spLFER's relate the partitioning coefficient to one physic-chemical property i.e., assume one process to determine the sorption process, while ppLFER's in principle account for all types of molecular interactions between solute and matrix (Goss and Schwarzenbach, 2001). The observed particulate mass fraction data, $\theta = c_p / (c_g + c_p)$ (Table 2), were tested with both a spLFER and a ppLFER model. The spLFER chosen is the widely used K_{oa} model of Finizio et al., 1997 (results presented in the Supplementary material (SM), S2.3). The ppLFER is a multi-phase model recently presented (Shahpoury et al., 2016) and applied for NPAHs (Tomaz et al., 2016). It is based on linear solvation energy relationships (Abraham, 1993; Goss, 2005):

(2) $\log K_p = eE + sS + aA + bB + lL + c$

(3) $\log K_p = sS + aA + bB + vV + lL + c$

where capital letters E, S, A, B, L, and V are solute-specific Abraham solvation parameters for excess molar refraction (describes interactions between π- and lone (n-) electron pairs), polarizability/ dipolarity, solute H-bond acidity, solute H-bond basicity, logarithm of solute hexadecane-air partitioning coefficient (unitless), and McGowan molar volume (cm^3 mol^{-1})/100, respectively (Endo and Goss, 2014). The corresponding parameters e, s, a, b, l, and v reflect matrix-specific solute-independent contribution to K_p. In lack of experimental data, the solute descriptors for NPAHs were taken from M.H. Abraham (personal communication). The multi-phase ppLFER considers adsorption onto soot, $(NH_4)_2SO_4$, and NH_4Cl, and absorption into particulate organic matter (OM). OM is assumed to be constituted of two separate phases, low to mid molecular mass, both organic soluble and water soluble OM. For these, ppLFER equations for dimethyl sulfoxide-air (representing the low molecular mass range) and for polyurethane ether-air (representing the high molecular mass OM) are used, respectively (Shahpoury et al., 2016).

A conventional single-parameter LFER (K_{oa}) model is applied, too.

2.4 Air mass history analysis

The HYSPLIT (Draxler and Rolph, 2003) and FLEXPART (Stohl et al., 1998, 2005) models were used to identify air mass histories over 10 and 2 days, respectively. The possible influence of polluted air on samples was quantified using a novel method of applying Lagrangian particle statistics (FLEXPART, see SM, S2.2). To this end, for the entire sampling period, one particle per second was released. The model output is generated at 0.062° (≈7 km), every 30 minutes and expressed as 'residence time' i.e., a measure of the time particles resided in grid cells. ECMWF meteorological data (0.125°×0.125° resolution, hourly) were used as input.

2.5 Quantification of urban influence on samples

The potential urban influence for individual samples collected at the marine site was based on the fraction of released Lagrangian particles which travelled through an urban boundary layer. A backward run from the sampling site was performed with Lagrangian particles (i.e. air parcels) being released during the entire sampling period. Three urban areas were considered, i.e. Izmir (≈300 km direct distance, 38.2-38.8°N/26.2-27.3°E), Athens (≈300 km, 37.8-38.1°N/23.5-23.8°E) and Istanbul (≈500 km away, 40.8-41.1°N/28.6-29.5°E).

The urban fractional dose, $D_{u\ i}$, an air mass collected in sample i had received for a given simulation period Δt can be derived as:

$$D_{u\,i} = \sum_t N_{blua}(t) \times \Delta t_{Rblua} / (N_{tot}(t) \times \Delta t_i) \quad (4)$$

with $N_{blua}(t)$ = number of virtual particles within the urban boundary layer during the specific time step, model output time resolution Δt_{Rblua} = 0.5 h, and $N_{tot}(t)$ = number of virtual particles present during the specific time step. Under the given flow conditions in the region, a 2-day time horizon is considered her. Hence, the simulation period is given as:

$$\Delta t_i = \Delta t_{sample} + 48h \quad (5)$$

253 with Δt_{sample} being the sampling time. $D_{u\ i}$ takes values between 0 and 1, corresponding to
254 none or all, respectively, of the entire sample air having crossed the urban boundary layer. The
255 D_u time series with allocation to 3 urban areas is shown in the SM, Fig. S3.

256 The comparison of urban influence in samples of various sample volume, V, requires
257 normalisation to V, a relative dose (equ. (5), with n = total number of samples collected).
258 Values of $D_{ru\ i}$ may exceed 1.

259

260 (6) $D_{ru\ i} = [\Sigma_n V_n/(nV_i)] \times D_{u\ i}$

261

262 The urban fractional dose, $D_{u\ i}$, accuracy is limited by the meteorological input data (here
263 0.125°×0.125° resolution, hourly) and boundary layer depth calculation. In the FLEXPART
264 model, the latter is done according to Vogelezang and Holtslag, 1996.

265

266 **3. Results and discussion**

267 The NPAH levels are distinctly lower at the marine than at the continental site, $\Sigma_{11\ 3\text{-}4r}$NPAH =
268 22.5 and 58.5 pg m^{-3}, respectively (Table 1). The NPAHs showing the highest concentrations
269 were 2NFLT and 3NPHE at the marine (Fig. 1b) and 9NANT and 2NFLT at the continental
270 site (Fig. 1d, Table 2). The substance patterns (composition of NPAH mixture) at both sites
271 are similar, though (R^2 = 0.76, P > 0.99, t-test). At the marine site, advection was northerly,
272 with air masses originating (time horizon 10 days) in eastern and central Europe and, towards
273 the end of the campaign, in the western Mediterranean. The site was placed into the
274 southeastern outflow of Europe. NO_x (0.2-0.6 ppbv), EC (0.2-0.8 µg m^{-3}) and PM_{10} (18.3-39.3
275 µg m^{-3}) reflect background conditions. Air mass history analysis suggests that the somewhat
276 elevated concentration in the first sample collected at the marine site (Fig. 1a) is related to
277 long-range transport influenced by passage over the urban areas of Izmir and Istanbul (urban
278 fractional dose D_u = 5.0%, in contrast to the mean which was 1.6%; Fig. S3). Overall, urban
279 fractional dose in the range <0.002–5.4% was received at the marine site. Across all samples
280 at the marine site, D_u is found to be significantly correlated with the pollutant sum
281 concentrations $\Sigma_{6\ 4r}$PAH and $\Sigma_{11\ 3\text{-}4r}$NPAH (R^2 = 0.61 and 0.69, respectively, both P > 0.99).

282 From the marine site data set, subsets of each two samples are formed, representing minimum
283 (i.e., almost no influence from industrialised area 48 hours prior to arrival (hereforth called

'marine background', urban fractional dose D_u = 0.4%) and maximum observed influence (hereforth called 'background with urban influence', D_u = 3.1%; SM Table S2, Figure S3). The results for these subsets are listed in Tables 1-3. Such classification was not deemed meaningful for the samples collected at the continental site, as the relevant source distribution in central Europe was too homogeneous during this episode. Advection was mostly from northwest and partly from easterly directions, with air mass origin (time horizon of 10 days) mostly in central Europe and, to a lesser extent in eastern Europe and the western Balkans. The NO_2 (1.2-2.6 ppbv), total carbon (3-6 µg m^{-3}) and PM_{10} (10.7-46.3 µg m^{-3}) levels during the campaign reflect continental background conditions.

The 4-ring PAH concentrations in samples from the continental site on the one hand, and in background air with urban influence collected at the marine site (urban areas 300-500 km away) on the other hand, are similar (Table 2). Also, the substance patterns are more similar than when relating all samples at the marine site i.e., R^2 = 0.88 (P > 0.999, t-test) instead of R^2 = 0.76. The investigation of the diffusive air-surface exchange processes during the measurements presented here showed that 4rPAHs were in fact influenced by secondary emissions, namely throughout day and night from the soil at the continental site (by average 16.3 and 9.3 pg m^{-2} h^{-1} for FLT and PYR, respectively; Degrendele et al., 2016) or occasionally from surface seawater at the marine site (during at least 1 day-time interval out of in total 3 of this data subset; Lammel et al., 2016). In the data set from the continental site, we study day/night (D/N) effects (subsets listed in Tables 1-3, too): PAH concentrations (c_{tot}) were ≈60% higher during the day than during the night, while c_{tot} of NPAH were by average ≈5% lower during the day (Table 2). NPAHs are subject to photolysis, while PAHs are not. At the site, the PAH concentrations were driven by re-volatilisation from soil, determined by temperature variation (Degrendele et al., 2016). For NPAHs (partly primary emitted) this indicates that the higher emissions during the day (due to re-volatilisation and road traffic) were compensated by shorter lifetime. NPAH lifetimes may be limited by heterogeneous photolysis, but available kinetic data are scarce and limited to few aerosol types (Fan et al., 1996; Feilberg and Nielsen, 2000, 2001; García-Berríos et al., 2017). Also, different NPAH/PAH ratios (the potential NPAH yields), which were 5.6% and 8.9% at the marine and continental sites, respectively, reflect the combination of emission sources and photochemical sinks. The NPAH/PAH ratios at the two sites were influenced by similar substance patterns upon emission, similar irradiation (summer, no or almost no clouds) and deposition velocities (θ in the range 0.05-0.20 for Σ_{11} 3-4rNPAH and Σ_6 4rPAH, no precipitation), but different re-

volatilisation fluxes and different characteristic transport times elapsed. Distance to major urban source areas was 300- >1000 km at the marine and 100-500 km at the continental site. The NPAH/PAH ratios being lower at the more distant receptor site, the marine site, may suggest that photochemical degradation of NPAHs along transport was on average faster than degradation of the precursors. xxx

The NPAH levels observed in marine background air are the lowest ever reported. Remarkably, the concentrations are much lower, by more than one order of magnitude, than one decade before at the same site during the same season (Tsapakis and Stephanou, 2007). The concentrations observed now are a factor of 4-10 lower than in a forest site in Amazonia two decades before (which might have been influenced by biomass burning emissions), a factor of 3 lower (for 2NPYR) than observed at an extremely remote site in the Himalayas two decades before (Ciccioli et al., 1996), and comparable to a high altitude site in the Alps (with the exception of 2NPYR which was observed one order of magnitude higher there in winter; Albinet et al., 2008a; Table 3). The NPAH levels observed at the marine site with influence of pollution and at the continental site are comparable, but also at the lower end of the range spanned by previous observations at rural and remote sites (Table 3).

Gas-particle partitioning

The time-weighted mean NPAH phase distributions (Σ_{11}3-4rNPAH) differ, corresponding to θ = 0.05 and 0.17 at the marine and continental sites, respectively, – despite similar temperatures (Table 1). In contrast and despite of similar temperature ranges, the 4-ring PAHs' ($\Sigma_6$4rPAH) particulate mass fraction was higher at the marine than at the continental site (θ = 0.42 and 0.20, respectively). Both 4-ring PAHs and 3-4 ring NPAHs were more associated with PM in polluted air than in clean air. This trend is weak for PAHs with θ = 0.02 for $\Sigma_6$4rPAH in marine background but 0.07 in background with urban influence (and θ = 0.09 and 0.20 for CHR; Table 2), but is obviously strong for NPAHs, namely θ = 0.19 for 2NPYR in marine background but 0.69 in background with urban influence, ≈0.93 in polluted continental air, and θ = 0.01 for Σ_{11}3-4rNPAH in marine background but 0.22 in background with urban influence (Table 2). The urban influenced air at the marine site is also reflected in a much higher OC (a factor of 3 higher than the all-campaign mean) and elevated EC, (less prominent, ≈50% above mean). This confirms the understanding that gas-particle partitioning

of both PAHs (Lohmann and Lammel, 2004; Shahpoury et al., 2016) and NPAHs (Tomaz et al., 2016) is mostly determined by absorption in POM and adsorption to soot. When comparing polluted air at the continental site and background with urban influence at the marine site, a strong shift of $\Sigma_6$4rPAH towards the particulate phase, $\theta \approx 0.21$ vs. 0.07, respectively, is found, while for Σ_{11}3-4rNPAH θ are similar i.e., ≈ 0.16 vs. 0.22, respectively. This phase partitioning trend of the 4rPAHs could be explained by sorption to EC, which is a factor of ≈2 higher, but not by OC (only ≈20% higher). In conclusion, these observations consistently indicate that sorption to soot is less significant for gas-particle partitioning of NPAHs than for PAHs.

While NPAHs were significantly phase-shifted ($\theta = 0.24$ during day-time but $\theta = 0.58$ during night-time), this was not the case for 4rPAHs ($\theta = 0.18$ during day-time and $\theta = 0.23$ during night-time). This is in line with the perception that the temperature sensitivity of phase change is stronger for the substance class with stronger molecular interactions in the condensed phase, NPAHs. E.g., the enthalpies of phase change between air and OC of FLT and NFLT are -98 and -75 kJ mol^{-1}, respectively (OC represented by DMSO; ACD, 2015).

Good agreement is found for the prediction of NPAH partitioning using the multi-phase (3-phase) ppLFER with most values predicted within one order of magnitude of the observed values (Fig. 2; quantification of deviations in S2.3.1). While the sensitivity of assumptions regarding PM phase composition, made in the model do not contribute significantly to the deviations (<< 1, log Kp units), a significant part can be attributed to the usage of estimated solute-specific Abraham solvation parameters (taken from ACD, 2015), in lack of experimentally based descriptors. E.g., for an urban site (Tomaz et al., 2016) it was found that experimentally based descriptors used for 9NPAH lead to better predictions than the estimated descriptors i.e., RMSEs differed by 0.43 log units. The agreement of the ppLFER prediction is better than assuming absorption (into OM) to be the only relevant process (K_{oa} model; see S2.3.2, Fig. S5). The same was found when studying gas-particle partitioning of NPAHs in urban air (Tomaz et al., 2016). This supports the perception that gas-particle partitioning of NPAHs is governed by various molecular interactions with OM, with its polarity being well represented by DMSO, better than by octanol. Earlier, it had been found for eight 3-4rNPAHs at urban and rural sites (Li et al., 2016) that the dual model, assuming adsorption (to soot) and absorption (into OM) predicts better than single adsorption (to the total aerosol surface i.e., Junge-Pankow) or single absorption (K_{oa}) models do.

The interactions with the aerosol matrix of 9NPHE (continental site) and 5NACE, 2NFLN, 2NFLT and 1NPYR (marine site) are less well represented than other NPAHs by the model as suggested by low slopes of their log $K_{p\ experimental}$/log $K_{p\ predicted}$ relationships. The reason is unknown. Moreover, sampling or sample handling artefacts cannot be excluded, even so same temperature range, sampler and sampling protocols applied across sites with both satisfactory and deficient agreement between predicted and observed K_p. Further conclusions are not supported by the limited amount of data and uncertainties on both the model (estimated ppLFER parameters) and experimental (concentrations close to LOQ) sides.

Mass size distribution

The NPAH mass size distribution had its maximum in the <0.49 µm size range at both sites. The 4-ring PAHs mass size distribution had 2 maxima, <0.49 µm and between 0.95 and 1.5 µm, at the marine site, but one at <0.49 µm at the continental site (Table 1). This is probably related to the presence of aged aerosol at the marine site vs. a larger contribution of fresh aerosols at the continental site. This is, furthermore, supported by the analysis of air mass origins that shows significant influence of urban areas for only few samples at the marine and for all samples at the continental site (SM S2).

Sums of NPAHs' and PAHs' mass size distributions are found unimodal with the maximum in particles <0.49µm, except PAHs at the marine site, which shows a second maximum between 1.5 and 3.0 µm (Fig. 3). At the marine site, 50 and 69% of 1NPYR and 2NFLT, respectively, were found associated with particles <0.45µm and 68 and 86%, respectively, with particles <0.95 µm, and even more, 83% and 100%, respectively, with particles <0.45µm at the continental site.

$\Sigma_6$4rPAH mass size distributions are shifted to larger particles in background with urban influence as compared to marine background air (both collected at the marine site) i.e., MMD = 0.19 and 0.28, respectively. However, such a trend is not apparent for NPAHs (Table 2). The size shift of PAHs is not corresponding to the PM_{10} mass size distribution: The MMD of PM_{10} for all samples collected at the marine site was 0.58 µm, while it was 1.13 and 0.62 µm in the marine background and background with urban influence data subsets, respectively. The PM_{10} as well as the OC mass size distributions were bimodal with maxima corresponding to < 0.49 µm and 3.0-7.2 µm particles (MMDs listed in Table 2), while the EC mass size distribution was unimodal, with the maximum concentration in the finest fraction. At the continental site, the Σ_{11}3-4rNPAH mass size distribution was bimodal with maxima corresponding to < 0.49

414 µm and 7.2-10 µm particles, while the $\Sigma_6$4rPAH mass size distribution was unimodal, with the
415 maximum concentration in the finest fraction (for all samples as well as for day and night data
416 subsets; Table 1).
417 The formation of a second maximum, at larger particles than emitted, reflects the
418 redistribution of semivolatile organics in an aged aerosol, hence, is expected at receptor sites
419 such as the marine site. This was also observed in polluted air, at rural and suburban sites, but
420 not at traffic sites or in winter at a rural site, when primary emissions dominated (unimodal;
421 Albinet et al., 2008b; Ringuet et al., 2012b).
422
423 **Substance patterns and NPAH formation during long-range atmospheric transport**
424 Among the targeted NPAHs and apart from NNAPs, which were highest concentrated,
425 2NFLT and 3NPHE prevailed at the marine site (accounting together for ≈60% of the NPAH
426 mass, excluding the NNAPs), while at the continental site 9NANT and 2NFLT prevailed
427 (accounting for ≈65% together) (Fig. 1, summarised in Fig. S4). The analytical method did not
428 separate the isomers 2NFLT and 3NFLT, but at receptor sites, far from diesel emissions it
429 appears justified to assume $c_{2NFLT} >> c_{3NFLT}$ (Finlayson-Pitts and Pitts, 2000; Zimmermann et
430 al., 2012). The ratio 1NPYR/2NPYR is higher, ≈1, at the continental site than at the marine
431 site (≈0.25), which reflects the significance of primary sources for polluted air (Atkinson and
432 Arey, 1994; Finlayson-Pitts and Pitts, 2000; Zimmermann et al., 2012). This ratio was found
433 similarly high or even higher at urban sites (Ringuet et al., 2012c; Tomaz et al., 2016).
434 Similarly, the ratio 2NFLT/1NPYR, the concentration of a secondarily formed over a primary
435 emitted NPAH, has been used as indicator for fresh emissions (if < 5) vs. photochemically
436 aged air mass (Keyte et al., 2013). These values were >> 5 in 21 out of 22 and 7 out of 8
437 samples at the marine and continental sites, respectively. The only sample collected at the
438 continental site with elevated primary NPAH (2NFLT/1NPYR = 4.3) was possibly influenced
439 by emissions from Budapest, which was passed by the advected air within the last hours
440 before arrival. The only sample collected at the marine site with elevated primary NPAH
441 (2NFLT/1NPYR = 5.9) was indeed directly influenced by emissions into the boundary layer
442 above the Izmir and Istanbul metropolitan areas (urban fractional dose D_u = 5.0% for samples
443 no. 1 and 2 in Fig. S3). In conclusion, these results from receptor / background sites confirm
444 the existing knowledge about primary emitted and secondarily formed NPAHs.
445 The ratio of two secondarily formed NPAHs, 2NFLT/2NPYR, indicative for day- vs. night-
446 time formation paths (Atkinson and Arey, 1994; Ciccioli et al., 1996), is found ≈2 at the

447 marine and ≈8 at the continental site (normalised to the precursor ratio i.e.,
448 2NFLT/2NPYR/(FLT/PYR); Table 4). Such low values point to day-time (OH initiated)
449 formation, while night-time (NO_3 initiated) formation was negligible, practically excluded at
450 the marine site. This is in line with the perception that NO_3 must have been very low in this
451 remote environment. (NO_x levels at the marine site were in the range 0.2-0.6 ppbv). A similar
452 conclusion had been drawn in a semi-rural environment (Feilberg et al., 2001).
453 For 2NFLT and 2NPYR (secondary sources only) and for 1NPYR, which has mostly primary
454 sources (Finlayson-Pitts and Pitts, 2000; Ringuet et al., 2012a; Jariyasopit et al., 2014a,
455 2014b) we infer the potential yields (Table 4). Here, yield is defined as c_{NPAH}/c_{PAH} (total
456 concentrations). This yield is called 'potential' as it reflects an upper estimate, as other PAH
457 photochemical sinks, such as formation of oxy-PAHs, are neglected. The yield of 2NFLT in
458 polluted air exceeds the one in background air only slightly, while the yield of 2NPYR in
459 polluted air exceeds the one in background air much more (a factor of 3 higher).
460 As expected, the highest potential yield of 1NPYR is found in polluted air (both sites),
461 reflecting the dominance of primary emissions of 1NPYR. Similarly, higher yields of
462 secondary NPAHs are found for marine background air compared to background air with
463 urban influence (marine site), reflecting the longer reaction times elapsed since PAH
464 emission. The yield for 2NFLT, c_{2NFLT}/c_{FLT}, ≈ 2-4% at both sites ranges higher than the one
465 for 2NPYR, c_{2NPYR}/c_{PYR}, which is found ≈ 0.5-2%. Note that because of the co-elution of
466 2NFLT and 3NFLT, and neglect of 3NFLT, the so derived values of c_{2NFLT}/c_{FLT} represent
467 actually upper estimates. Apart from sites which were immediately influenced by PAH sources
468 (road traffic, power plant, biomass burning), only very few studies reported NPAH together
469 with precursor data in both phases of ambient air. c_{2NPYR}/c_{PYR} = 1.0%, similar to our finding at
470 remote sites, but a very high c_{2NFLT}/c_{FLT} = 12.9% were reported from a suburban site in France
471 in summer during day-time (corresponding values for night-time were 2.0 and 9.4%,
472 respectively; Ringuet et al., 2012c). 2NFLT was not separated from 3NFLT (similar to our
473 data set). A suburban site will be influenced by direct 3NFLT emissions, such that c_{2NFLT}/c_{FLT}
474 is an upper estimate. Much lower ratios, c_{2NFLT}/c_{FLT} = 0.20% and c_{2NPYR}/c_{PYR} = 0.08% were
475 reported as the median values for 90 sites of various categories, rural and urban, in northern
476 China in summer (Lin et al., 2015). These yields are somewhat higher for the subset of the
477 rural sites. The potential yields found at the marine site in our study are close to the yields for
478 OH-initiated photochemistry observed in laboratory experiments under high NO_x conditions
479 i.e., 3% for c_{2NFLT}/c_{FLT} and 0.5% for c_{2NPYR}/c_{PYR} (Atkinson and Arey, 1994).

4. Conclusions

For the first time pollution contained in individual background air samples was quantified, by means of a fractional dose. The fractional dose indicated how much the collected volume of air had been exposed to an urban boundary layer within a given time horizon. This is found suitable to discriminate among samples and discuss results, clearly beyond qualitative reasoning on back trajectories alone. The concept could be applied to any type of georeferenced origin and might be useful to track the influence of land use of various kind, or ship and aircraft routes.

Our measurements confirmed occurrence of mutagenic NPAHs, earlier reported from polluted atmospheric environments of America, Europe and Asia, also for the European background atmosphere and the outflow of Europe. These substances obviously go into intercontinental transport and might be indeed ubiquitous. The mass size distribution is determined by the particle size upon emission (primary NPAHs) and condensation and redistribution in the aerosol along transport, hence, does not include the short-lived coarse mass fraction. This indicates a high long-range transport potential. However, the observation of 3.8 and 0.92 pg m^{-3} of 2NFLT and 2NPYR, respectively, measured at the southeastern outflow of Europe (the lowest ever reported concentrations; Table 3), may indicate that their abundance in the remote global environment could be less than anticipated. Earlier, this was based on a single measurement of 2NPYR, 3 pg m^{-3}, at an extremely remote site in central Asia two decades before (Ciccioli et al., 1996). Moreover, this air, classified as marine background, was not completely clean, but had been exposed to a non-zero fractional urban pollution dose (0.4% of the total, time horizon of 2 days). More measurements at remote sites should verify NPAH levels globally. PAHs have been abated significantly in Europe during the last decades (EEA, 2014), which should also be reflected in long-term trends of their derivatives. However, a temporal trend for the Aegean or the southeastern outflow of Europe in summer cannot be inferred based on the current and the earlier (2002; Tsapakis and Stephanou, 2007) campaign data. NPAHs should be included in monitoring programmes to better assess the exposure of human health hazards of atmospheric pollution, even in remote areas.

Understanding of NPAH formation in ambient air is still rudimentary. Although our observations of a potential NPAH yield are in agreement with laboratory studies of OH-initiated photochemistry, the kinetics of NPAHs, both formation from parent PAHs and

photolysis remains to be quantitatively studied under relevant conditions for the background atmosphere i.e., low NO_x and on various aerosol matrices including sea salt, respectively. More studies into NPAH atmospheric fate, both field observations and kinetic data, are needed in order to assess and quantify spatial and temporal trends, the long-range transport potential and persistence.

Acknowledgements

We thank Christos I. Efstathiou (Masaryk University), András Hoffer, Gyula Kiss (MTA-PE Air Chemistry Research Group, Veszprém), Jiři Kohoutek (MU), Giorgos Kouvarakis (University of Crete, Iraklion) and Lajos Szöke (Hungarian Meteorological Service) for on-site support, Giorgos Kouvarakis and Krisztina Labancz (Hungarian Meteorological Service) for meteorological and trace gas data, Michael H. Abraham (University College London) for providing ppLFER solute descriptors, Ignacio Pisso (NILU, Kjeller, Norway) for model post-processing scripts and Céline Degrendele (MU) and Manolis Tsapakis (Hellenic Centre for Marine Research, Gournes) for discussion. This research was supported by the Czech Science Foundation (n° P503 16-11537S), the Czech Ministry of Education, Youth and Sports (n° LO1214 and LM2015051), and the European Union FP7 (n° 262254, ACTRIS).

Compliance with Ethical Standards No potential conflicts of interest (financial or non-financial) exist.

References

Abraham, M.H.: Scales of solute hydrogen-bonding: their construction and application to physicochemical and biochemical processes. Chem. Soc. Rev., 22, 73–83, 1993.

ACD: ACD/Labs Absolv Software, Advanced Chemistry Development, Toronto, Canada, 2015.

Albinet, A., Leoz-Garziandia, E., Budzinski, H., and ViIlenave, E.: Simultaneous analysis of oxygenated and nitrated polycyclic aromatic hydrocarbons on standard reference material 1649a (urban dust) and on natural ambient air samples by gas chromatography-mass spectrometry with negative ion chemical ionisation. J. Chrom. A, 1121, 106-113, 2006.

Albinet, A., Leoz-Garziandia, E., Budzinski, H., and ViIlenave, E.: Polycyclic aromatic hydrocarbons (PAHs), nitrated PAHs and oxygenated PAHs in ambient air of the Marseilles area (South of France): Concentrations and sources. Sci. Total Environ., 384, 280-292, 2007.

Albinet, A., Leoz-Garziandia, E., Budzinski, H., Villenave, E., and Jaffrezo, J.L.: Nitrated and oxygenated derivatives of polycyclic aromatic hydrocarbons in the ambient air of two French alpine valleys part 1: concentrations, sources and gas/particle partitioning. Atmos. Environ., 42, 43-54, 2008a.

Albinet, A., Leoz-Garziandia, E., Budzinski, H., Villenave, E., and Jaffrezo, J.L.: Nitrated and oxygenated derivatives of polycyclic aromatic hydrocarbons in the ambient air of two French alpine valleys part 2: Particle size distribution. Atmos. Environ., 42, 55-64, 2008b.

Alves, C.A., Vicente, A.M.P., Gomes, J., Nunes, T., Duarte, M., and Bandowe, B.A.M.: Polycyclic aromatic hydrocarbons (PAHs) and their derivatives (oxygenated-PAHs, nitrated-PAHs and azaarenes) in size-fractionated particles emitted in an urban road tunnel. Atmos. Res., 180, 128-137, 2016.

Arey, J.: Atmospheric reactions of of PAHs including formation of nitro-arenes. In: The handbook of Environmental Chemistry, Vol. 3I: PAHs and Related Compounds (Neilson AH, ed.), Springer, Berlin, pp. 347-385, 1998.

Arey, J., Atkinson, R., Zielinska, B., and McElroy, P.A.: Diurnal concentrations of volatile polycyclic aromatic hydrocarbons and nitroarenes during a photochemical air pollution episode in Glendora, California. Environ. Sci. Technol., 23, 321-327, 1989.

Atkinson, R., and Arey, J.: Atmospheric chemistry of polycyclic aromatic hydrocarbons: Formation of atmospheric mutagens. Environ. Health Persp., 102, 117-126. 1994.

Bamford, H.A., and Baker, J.E.: Nitro-polycyclic aromatic hydrocarbon concentrations and sources in urban and suburban atmospheres of the Mid-Atlantic region. Atmos. Environ., 37, 2077-2091, 2003.

Barrado, A.I., García, S., Sevillano, M.L., Rodríguez, J.A., and Barrado, E.: Vapor-phase concentrations of PAHs and their derivatives determined in a large city: Correlations with their atmospheric aerosol. Chemosph., 93, 1678-1684, 2013.
Borbély-Kiss, I., Haszpra, L., Koltay, E., László, S., Mészáros, A., Mészáros, E., and Szabó, S.: Elemental concentrations and regional signatures in atmospheric aerosols over Hungary. Physica Scripta, 37, 299-304, 1988.
Ciccioli, P., Cecinato, A., Brancaleoni, E., Frattoni, M., Zacchei, P., Miguel, A., and de Castro Vasconcellos, P.: Formation and transport of 2-nitrofluoranthene and 2-nitropyrene of photochemical origin in the troposphere. J. Geophys. Res., 101, 19567-19582, 1996.
Claxton, L.D., Matthews, P.P., and Warren, S.H.: The genotoxicity of ambient outdoor air, a review: Salmonella mutagenicity, Mutation Res. Rev. 567, 347-399, 2004.
Degrendele, C., Audy, O., Hofman, J., Kučerik, J., Kukučka, P., Mulder, M.D., Přibylová, P., Prokeš, R., Šáňka, M., Schaumann, G.E., and Lammel, G.: Diurnal variations of air-soil exchange of semi-volatile organic compounds (PAHs, PCBs, OCPs and PBDEs) in a central European receptor area. Environ. Sci. Technol., 50, 4278–4288, 2016.
Draxler, R.R., and Rolph, G.D.: HYSPLIT (HYbrid Single-Particle Lagrangian Integrated Trajectory) Model access via NOAA ARL READY. NOAA Air Resources Laboratory, Silver Springs, USA. 2003, Available from: http://www.arl.noaa.gov/ready/hysplit4.html.
EEA: European emission inventory report 1990-2012 under the UNECE Convention on Long-range Transboundary Air Pollution (LRTAP), European Environment Agency Technical Report No. 12/2014, Copenhagen, 2014, 132 pp.
EMEP: Transboundary particulate matter, photo-oxidants, acidifying and eutrophying components. Co-operative Programme for Monitoring and Evaluation of the Long-range Transmission of Air Pollutants in Europe, EMEP Report No. 1/2015, Oslo, 150+78 pp. Available from: http://emep.int/publ/reports/2015/EMEP_Status_Report_1_2015.pdf, 2015
Endo, S., and Goss, K.U.: Applications of poly-parameter linear free energy relationships in environmental chemistry. Environ. Sci. Technol., 48, 12477–12491, 2014.
Fan, Z.H., Kamens, R.M., Hu, J.X., Zhang, J.B., and McDow, S.: Photostability of nitro-polycyclic aromatic hydrocarbons on combustion soot particles in sunlight. Environ. Sci. Technol., 30, 1358–1364, 1996.
Feilberg, A., and Nielsen, T.: Effect of aerosol chemical composition on the photodegradation of nitro-PAHs. Environ. Sci. Technol., 34, 789-797, 2000.
Feilberg, A., and Nielsen, T.: Photodegradation of nitro-PAHs in viscous organic media used as models of organic aerosols. Environ. Sci. Technol., 35, 108-113, 2001.
Feilberg, A., Poulsen, M.W.B., Nielsen, T., and Skov, H.: Occurrence and sources of particulate nitro polycyclic aromatic hydrocarbon in ambien air in Denmark. Atmos. Environ., 35, 353-366, 2001.
Finizio, A., Mackay, D., Bidleman, T., and Harner, T.: Octanol-air partition coefficient as a predictor of partitioning of semi-volatile organic chemicals to aerosols. Atmos. Environ., 31, 2289–2296, 1997.
Finlayson-Pitts, B.J., and Pitts, J.N.: Chemistry of the Upper and Lower Atmosphere: Theory, Experiments, Application, San Diego (Academic Press), USA, 2000
García-Berríos, Z.I., Arce, R., Burgos-Martínez, M., and Burgos-Polanco, N.D.: Phototransformations of environmental contaminants in models of the aerosol: 2 and 4-nitropyrene. J. Photochem. Photobiol. A, 332, 131-140, 2017.
Garner, R.C., Stanton, C.A., Martin, C.N., Chow, F.L., Thomas, W., Hübner, D., and Herrmann, R.: Bacterial mutagenicity and chemical analysis of polycyclic aromatic hydrocarbons and some nitro derivatives in environmental samples collected in West Germany. Environ Mutagen, 8, 109-117, 1986.
Goss, K.U.: Predicting the equilibrium partitioning of organic compounds using just one linear solvation energy relationship (LSER). Fluid Phase Equilib., 233, 19–22, 2005.
Goss, K.U., and Schwarzenbach, R.P.: Linear free energy relationships used to evaluate equilibrium partitioning of organic compounds. Environ. Sci. Technol., 35, 1–9, 2001.
Grosjean, D., Fung, K., and Harrison, J.: Interactions of polycyclic aromatic hydrocarbons with atmospheric pollutants. Environ. Sci. Technol., 17, 673–679, 1983.
Halsall, C.J., Sweetman, A.J., Barrie, L.A., and Jones, K.C.: Modelling the behaviour of PAHs during atmospheric transport from the United Kingdom to the Arctic. Atmos. Environ. 35, 255-267.
Hayakawa, K. (2016) Environmental behaviors and toxicities of polycyclic aromatic hydrocarbons and nitropolycyclic aromatic hydrocarbons. Chem. Pham. Bull., 64, 83-94, 2001.
Inomata, S., Fushimi, A., Sato, K., Fujitani, Y., and Yamada, H.: 4-Nitrophenol, 1-nitropyrene, and 9-nitroanthracene emissions in exhaust particles from diesel vehicles with different exhaust gas treatments. Atmos. Environ., 110, 93-102, 2015.
Jaenicke, R.: Aerosol physics and chemistry. Landolt-Börnstein Neue Serie b, 4, 391–457, 1988.

Jariyasopit, N., Zimmermann, K., Schrlau, J., Arey, J., Atkinson, R., Yu, T.W., Dashwood, R.H., Tao, S., and Massey Simonich, S.L.: Novel NPAH formation from heterogeneous reactions of PAHs with NO_2, NO_3/N_2O_5, OH radicals, and OH radicals: Prediction, laboratory studies and mutagenicity. Environ. Sci. Technol., 48, 412-419, 2014a.

Jariyasopit, N., Zimmermann, K., Schrlau, J., Arey, J., Atkinson, R., Yu, T.W., Dashwood, R.H., Tao, S., and Massey Simonich, S.L.: Heterogeneous reactions of particulate matter-bound PAHs and NPAHs with NO_3/N_2O_5, OH radicals, and O_3 under simulated long-range atmospheric transport conditions: Reactivity and mutagenicity. Environ. Sci. Technol., 48, 10155-10164, 2014b.

Keyte, I.J., Harrison, R.M., and Lammel, G.: Chemical reactivity and long-range transport potential of polycyclic aromatic hydrocarbons – a review. Chem. Soc. Rev., 42, 9333-9391, 2013.

Keyte, I.J., Albinet, A., and Harrison, R.M.: On-road traffic emissions of polycyclic aromatic hydrocarbons and their oxy- and nitro- derivative compounds measured in road tunnel environments. Sci. Total Environ., 566-567, 1131-1142, 2016.

Kouvarakis, G., Tsigaridis, K., Kanakidou, M., and Mihalopoulos, N.: Temporal variations of surface regional background ozone over Crete Island in the Southeast Mediterranean. J. Geophys. Res., 105, 4399-4407, 2000.

Lafontaine, S., Schrlau, J., Butler, J., Jia, Y.L., Harper, B., Harris, S., Bramer, L.M., Waters, K.M., Harding, A., and Massey Simonich, S.L.: Relative influence of trans-Pacific and regional atmospheric transport of PAHs in the Pacific Northwest, U.S. Environ. Sci. Technol., 49, 13807-13816, 2015.

Lammel, G., Audy, O., Besis, A., Efstathiou, C., Eleftheriadis, K., Kohoutek, J., Kukučka, P., Mulder, M.D., Přibylová, P., Prokeš, R., Rusina, T., Samara, C., Sofuoglu, A., Sofuoglu, S.C., Taşdemir, Y., Vassilatou, V., Voutsa, D., and Vrana, B.: Air and seawater pollution and air-sea gas exchange of persistent toxic substances in the Aegean Sea: spatial trends of PAHs, PCBs, OCPs and PBDEs. Environ. Sci. Pollut. Res., 22, 11301-11313, 2015.

Lammel, G., Meixner, F.X., Vrana, B., Efstathiou, C., Kohoutek, J., Kukučka, P., Mulder, M.D., Přibylová, P., Prokeš, R., Rusina, T.S., Song, G.Z., and Tsapakis, M.: Bi-directional air-sea exchange and accumulation of POPs (PAHs, PCBs, OCPs and PBDEs) in the nocturnal marine boundary layer. Atmos. Chem. Phys., 16, 6381-6393, 2016.

Li, W., Shen, G.F., Yuan, C.Y., Wang, C., Shen, H.Z., Jiang, H., Zhang, Y.Y., Chen, Y.C., Su, S., Lin, N., and Tao, S.: The gas/particle partitioning of nitro- and oxy-polycyclic aromatic hydrocarbons in the atmosphere of northern China. Atmos. Res., 172-173, 66-73, 2016.

Lin, Y., Qiu, X.H., Ma, Y.Q., Ma, J., Zheng, M., and Shao, M.: Concentrations and spatial distribution of polycyclic aromatic hydrocarbons (PAHs) and nitrated PAHs (NPAHs) in the atmosphere of North China, and the transformation from PAHs to NPAHs. Environ. Pollut., 196, 164-170, 2015.

Lohmann, R., and Lammel, G.: Adsorptive and absorptive contributions to the gas particle partitioning of polycyclic aromatic hydrocarbons: State of knowledge and recommended parameterisation for modelling, Environ. Sci. Technol., 38, 3793-3803, 2004.

Masclet, P., Pistikopoulos, P., Beyne, S., and Mouvier, G.: Long-range transport and gas/particle distribution of polycyclic aromatic hydrocarbons at a remote site in the Mediterranean sea, Atmos. Environ., 22, 639-650, 1988.

Melymuk, L., Bohlin-Nizzetto, P., Prokeš, R., Kukučka, P., and Klánová, J.: Sampling artifacts in active air sampling of semivolatile organic contaminants: Comparing theoretical and measured artifacts and evaluating implications for monitoring networks. Environ. Pollut., 217, 97-106, 2016.

Mihalopoulos, N., Stephanou, E., Pilitsidis, S., Kanakidou, M., and Bousquet, P.: Atmospheric aerosol composition above the Eastern Mediterranean region. Tellus B, 49, 314-326, 1997.

Nielsen, T., Seitz, B., and Ramdahl, T.: Occurrence of nitro-PAH in the atmosphere in a rural area. Atmos. Environ., 18, 2159-2165, 1984.

Pandis, S.N., Baltensperger, U., Wolfenbarger, J.K., and Seinfeld, J.H.: Inversion of aerosol data from the epiphaniometer. J. Aerosol Sci., 22, 417-428, 1991.

Pankow, J.F.: Overview of the gas phase retention volume behaviour of organic compounds on polyurethane foam. Atmos. Environ., 23, 1107-1111, 1989.

Pitts, J.N., Arey, J., Zielinska, B., Winer, A.M., and Atkinson, R.: Determination of 2-nitro-fluoranthene and 2-nitropyrene in ambient particulate organic matter: Evidence for atmospheric reactions. Atmos. Environ., 19, 1601-1608, 1985.

Ramdahl, T., Zielinska, B., Arey, J., Atkinson, R., Winer, A.M., and Pitts, J.N.: Ubiquitous occurrence of 2-nitro-fluoranthene and 2-nitropyrene in air. Nature, 321, 425-427, 1986.

Reisen, F., and Arey, J.: Atmospheric reactions influence seasonal PAH and nitro-PAH concentrations in the Los Angeles Basin. Environ. Sci. Technol., 39, 64-73, 2005.

Ringuet, J., Albinet, A., Leoz-Garziandia, E., Budzinski, H., and Villenave, E.: Reactivity of polycyclic aromatic compounds (PAHs, NPAHs and OPAHs) adsorbed on natural aerosol particles exposed to atmospheric oxidants. Atmos. Environ., 61, 15–22, 2012.

Ringuet, J., Leoz-Garziandia, E., Budzinski, H., Villenave, E., and Albinet, A.: Particle size distribution of nitrated and oxygenated polycyclic aromatic hydrocarbons (NPAHs and OPAHs) on traffic and suburban sites of a European megacity: Paris (France). Atmos. Chem. Phys., 12, 8877-8887, 2012b.

Ringuet, J., Albinet, A., Leoz-Garziandia, E., Budzinski, H., and Villenave, E.: Diurnal/nocturnal concentrations and sources of particulate-bound PAHs, OPAHs and NPAHs at traffic and suburban sites in the region of Paris (France), Sci. Total Environ., 437, 297-305, 2012c.

Schauer, C., Niessner, R., and Pöschl, U.: Analysis of nitrated polycyclic aromatic hydrocarbons by liquid chromatography with fluorescence and mass spectrometry detection: air particulate matter, soot, and reaction product studies. Anal. Bioanal. Chem., 378, 725-736, 2004.

Schuetzle, D.: Sampling of vehicle emissions for chemical analysis and biological testing. Environ. Health Perspect., 47, 65-80, 1983.

Shahpoury, P., Lammel, G., Albinet, A., Sofuoğlu, A., Dumanoğlu, Y., Sofuoğlu, S.C., Wagner, Z., and Ždimal, J.: Model evaluation for gas-particle partitioning of polycyclic aromatic hydrocarbons in urban and non-urban sites in Europe – Comparison between single- and poly-parameter linear free energy relationships based on a multi-phase aerosol scenario. Environ. Sci. Technol., 50, 12312-12319, 2016.

Stohl, A., Hitzenberger, M., and Wotawa, G.: Validation of the Lagrangian particle dispersion model FLEXPART against large scale tracer experiments. Atmos. Environ., 32, 4245-4264, 1998.

Stohl, A., Forster, C., Frank, A., Seibert, P., and Wotawa, G.: Technical note: The Lagrangian particle dispersion model FLEXPART version 6.2. Atmos. Chem. Phys., 5, 2461-2474, 2005.

Tomaz, S., Shahpoury, P., Jaffrezo, J.L., Lammel, G., Perraudin, E., Villenave, E., and Albinet, A.: One year study of polycyclic aromatic compounds at an urban site in Grenoble (France): seasonal variations, gas/particle partitioning and cancer risk estimation, Sci. Total Environ., 565, 1071-1083, 2016.

Tsapakis, M., and Stephanou, E.G.: Diurnal cycle of PAHs, nitro-PAHs and oxy-PAHs in a high oxidant capacity marine background atmosphere. Environ. Sci. Technol., 41, 8011-8017, 2007.

Vincenti, M., Maurino, V., Minero, C., and Pelizzetti, E.: Determination of nitro-substituted polycyclic aromatic hydrocarbons in the Antarctic airborne particulsate. Intl. J. Environ. Anal. Chem., 79, 257-272, 2001.

Vogelezang, D. H. P., and Holtslag, A. A. M.: Evaluation and model impacts of alternative boundary-layer height formulations. Bound.-Layer Met., 81, 245–269, 1996.

Vrekoussis, M., Liakakou, E., Kocak, M., Kubilay, N., Oikonomou, K., Sciare, J., and Mihalopoulos, N. (2005) Seasonal variability of optical properties of aerosols in the Eastern Mediterranean, Atmos. Environ. 39, 7083-7094.

Yamasaki, H., Kuwata, K., and Miyamoto, H.: Effects of ambient temperature on aspects of airborne polycyclic aromatic hydrocarbons. Environ. Sci. Technol., 16, 189–194, 1982.

Zimmermann, K., Atkinson, R., Arey, J., Kojima, Y., and Inazu, K.: Isomer distributions of molecular weight 247 and 273 nitro-PAHs in ambient samples, NIST diesel SRM, and from radical-initiated chamber reactions. Atmos. Environ., 55, 431-439, 2012.

Zimmermann, K., Jariyasopit, N., Massey Simonich, S.L., Tao, S., Atkinson, R., and Arey, J.: Formation of NPAHs from the heterogeneous reaction of ambient particle-bound PAHs with $N_2O_5/NO_3/NO_2$. Environ. Sci. Technol., 47, 8434-8442, 2013.

719 Table 1. Overview time weighted mean concentrations in the particulate and gas phases, and
720 ambient temperature. Data subsets (B = background, P = polluted, D = day mean, N = night
721 mean) and mass size distribution (<0.45/0.45-0.95/0.95-1.5/1.5-3.0/3.0-7.2/7.2-10 µm
722 aerodynamic equivalent diameter) in brackets.

Site	Phase	Σ_{11} 3-4rNPAH (pg m^{-3})	Σ_{6} 4rPAH (pg m^{-3})
Marine	particulate (n = 8)	4.1 (3.5/0.6/0.2/0.03/0.03/0.00) (B: 0.2/P: 8.7)	43 (28/8.1/1.2/6.2/4.3/1.7) (B: 7.9/P: 42.4)
	gas (n = 21)	18.4 (B: 13.2/P:31.1)	403 (B:321/P:580)
	T(°C)	25.6 (B: 27.1/P: 22.0)	
Continental	particulate (n = 22)	24.3 (20.5/2.9/0.7/0.04/0.06/0.15) (D:13.9/N:34.6)	129 (87/28/12/0.6/0.0/0.0) (D:146/N:116)
	gas (n = 22)	34.2 (D:42.9/N:25.5)	517 (D:649/N:384)
	T(°C)	23.1 (D:28.8/N:17.5)	

723

724

725 Table 3. Comparison of total (g + p) concentrations in air, c_{tot} (pg/m^3), with other
726 measurements at remote and rural sites

	1NPYR (pg/m^3)	2NFLT (pg/m^3)	2NPYR (pg/m^3)	References
background CEu summer 2013	1.1	15 [a]	1.3	this work (continental)
E Mediterranean summer 2012	0.74	8.6 [a]	2.5	this work (marine)
E Mediterranean clean summer 2012	0.21	3.8 [a]	0.92	this work (marine background [b])
E Mediterranean clean summer 2002	-	29	21	Tsapakis and Stephanou, 2007
Ross Sea coast, Antarctica	<0.02 [c]	<0.03 [c]		Vincenti et al., 2001
Himalayas, Nepal 1991	-	-	3	Ciccioli et al., 1996
Forest Amazonia 1993	2	15	8	
Rural Northern Germany 1991	-	-	3	
Rural Denmark winter-spring 1982	9±5 [c]	-	-	Nielsen et al., 1984
Semi-rural Denmark all year 1998-99	40	97	6.3	Feilberg et al., 2001
Remote Alps 2002	2.2	-	-	Schauer et al., 2004
Rural Alps 2002	6.6	-	-	
Rural Alps [d] winter 2002-03	21	96 [a]	81	Albinet et al., 2008a
Rural Alps [d] summer 2003	4.2	28 [a]	5.7	
Remote Alps [e] winter 2002-03	2.4	1.3 [a]	14.8	
Remote Alps [e] summer 2003	0.6	1.8 [a]	0.7	
Rural Southern France 2004	0.6	2.6 [a]	1.6	Albinet et al., 2007

727 [a] co-eluted with 3NFLT, assuming $c_{3NFLT} = 0$
728 [b] samples No. 9, 10, 19 and 22 in Fig. S3
729 [c] particulate phase concentration only
730 [d] Val de Maurienne sites (Albinet et al., 2008a)
731 [e] Plan de l'Aiguille site (Albinet et al., 2008a)
732

Table 4: Selected 4-ring PAHs and primary and secondary 3-4 ring NPAH total (g + p) time-weighted mean concentrations ±σ (pg m^{-3}). Potential yields, c_{NPAH}/c_{PAH}, in brackets. σ given for n > 2.

Site		Marine			Continental
	Data subset	all (n = 8[a])	marine background (n = 2[b])	background with urban influence (n = 2[c])	all (n = 22)
Primary	FLT	213±161	161	259	342±215
	PYR	146±130	103	188	226±131
Primary and secondary (potential yield)	2NFLN [d]	0.038±0.12	<0.18	0.15	0.034±0.044
	1NPYR	0.62±1.1 (0.4±0.2%)	0.21 (0.2%)	1.4 (0.7%)	1.1±0.6 (0.6±0.3%)
Secondary (yield)	2NFLT [e]	7.7±8.5 (3.6±2.0%)	1.68 (1.0%)	11.0 (4.2%)	15±10 (6.5±7.5%)
	2NPYR	2.2±2.6 (1.5±0.7%)	0.92 (0.9%)	3.3 (1.8%)	1.3±1.7 (0.74±1.09%)

[a] 8 filter and 21 PUF samples
[b] 2 filter and 6 PUF samples i.e., No. 9-10 and 19-22 in Fig. S3 (urban fractional dose D_u = 0.4%)
[c] 2 filter and 5 PUF sample i.e., No. 1-2 and 15-18 in Fig. S3 (D_u = 3.1%)
[d] no yield given as c_{FLN} not quantified
[e] co-eluted with 3NFLT, assuming $c_{3NFLT} = 0$

Fig. 1: Time series of absolute (a, c; pg m^{-3}) and relative (b, d) total (gas + particulate) NPAH concentrations at the (a, b) marine (24 h means shown [a]) and (c, d) continental site (day / night means)

a. b.

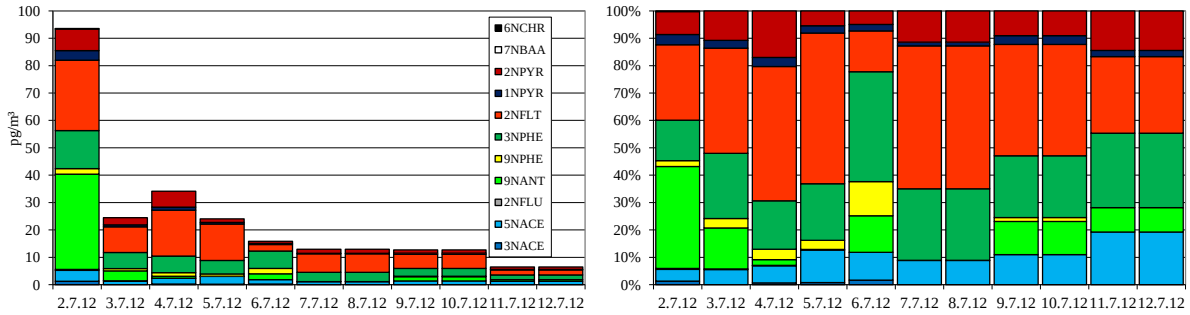

c. d.

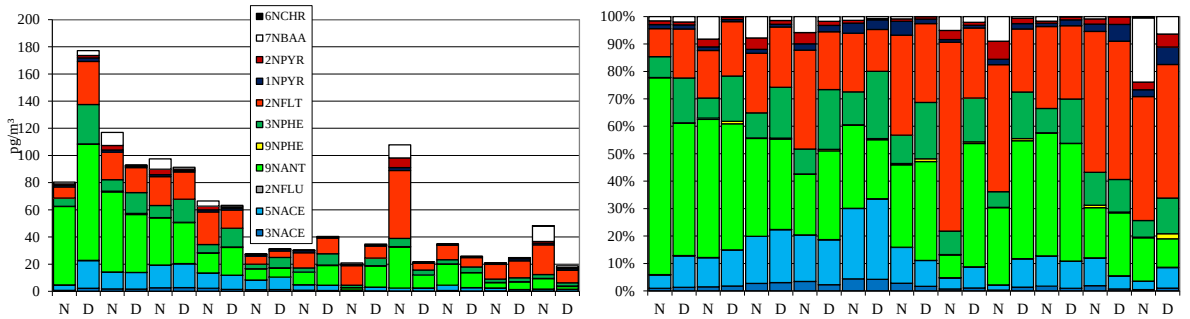

[a] gas-phase (PUF) sampled day / night, particulate phase (filter) sampled 1-4 subsequent days / nights, 4 during the period 7.-12.7.12

753 Fig. 2: Predicted versus experimental log K_p (m^3 air g^{-1} PM) for NPAHs using the multi-phase
754 ppLFER model at the (a) marine and (b) continental site

755 a.

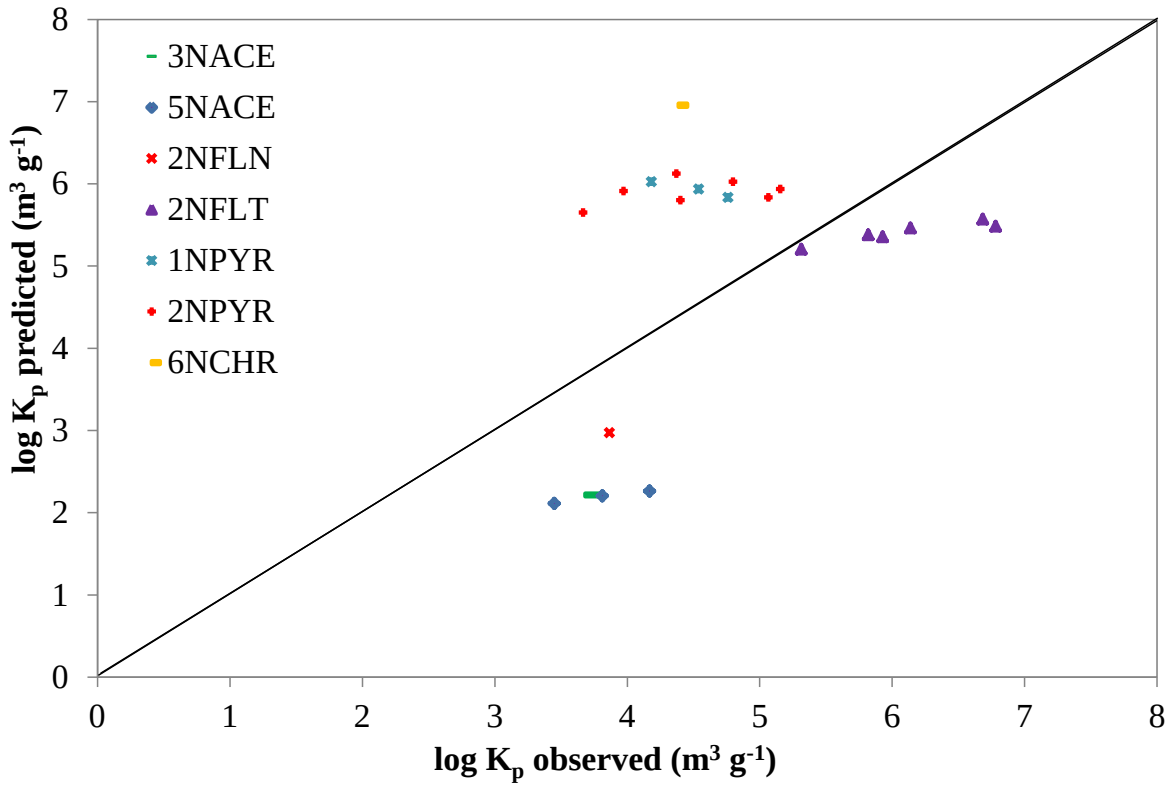

756

757 b.

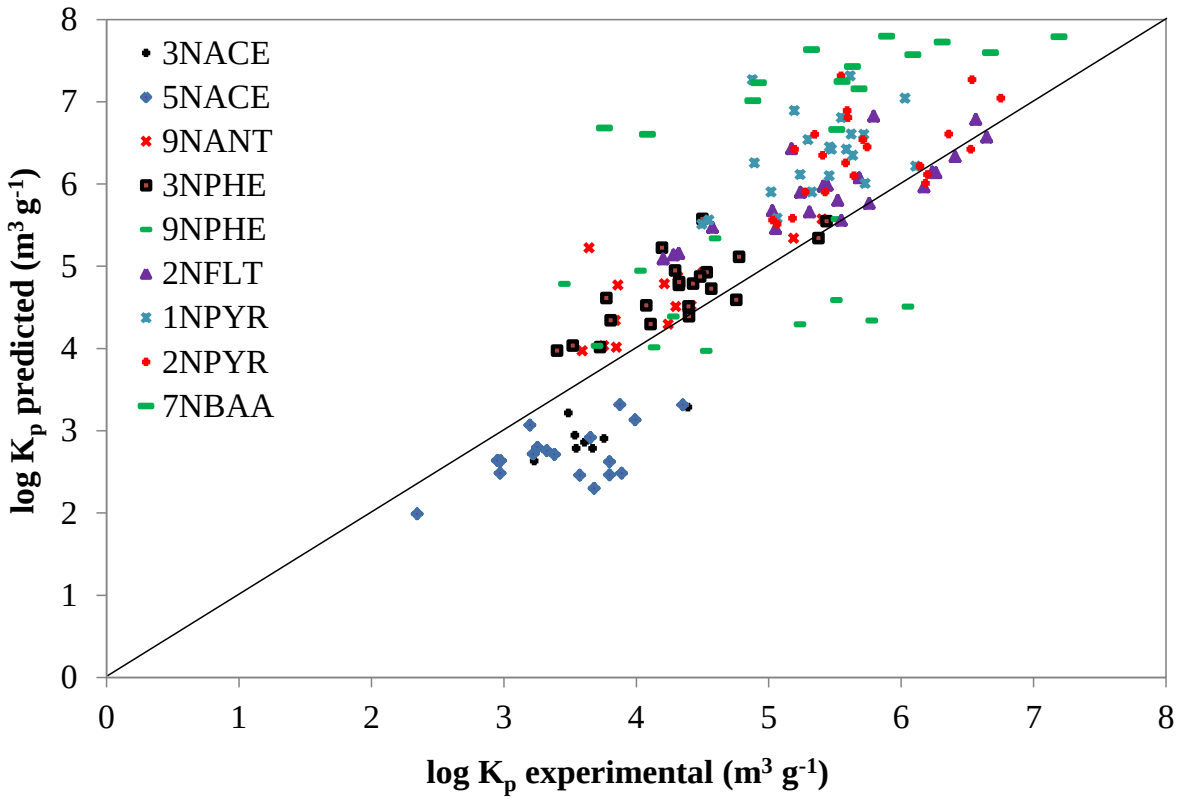
3NACE
5NACE
9NANT
3NPHE
9NPHE
2NFLT
1NPYR
2NPYR
7NBAA
log Kp predicted (m3 g-1)
log Kp experimental (m3 g-1)
0
1
2
3
4
5
6
7
8

758
759
760

761 Fig. 3. Time-weighted mean $\Sigma_6$4rPAH and Σ_{11}3-4rNPAH mass size distributions (pg m^{-3}) at
762 the marine and continental sites. The error bars show the standard deviation from the
763 campaign mean.

Site	PAH	NPAH
Marine	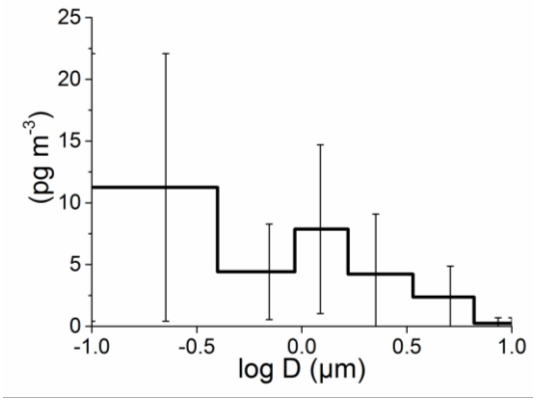	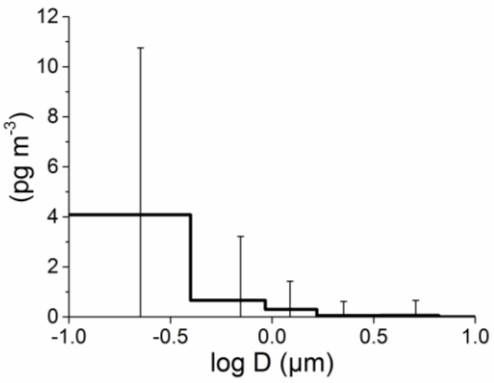
Continental	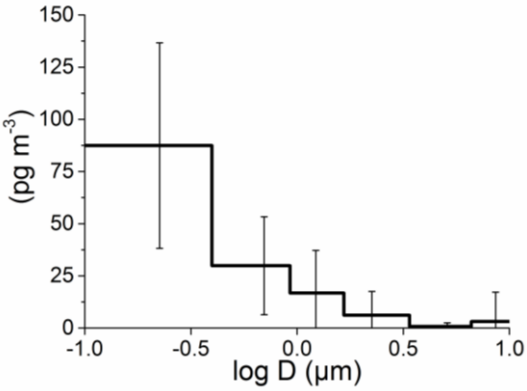	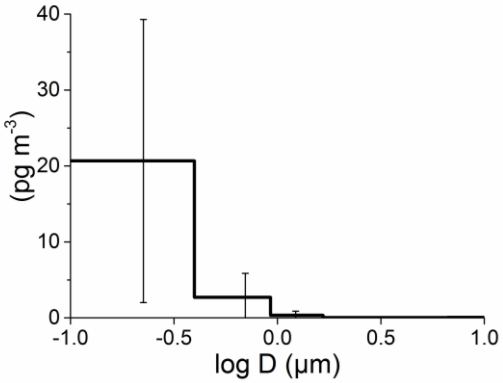

764

765

Table 2. Total (g + p) time-weighted concentrations, c_{tot} (pg m^{-3}), particulate mass fraction, $\theta = c_p / c_{tot}$, and mass median diameter (MMD, µm), of of 2-4-ring NPAHs and 4-ring PAHs at the marine (as 'mean (background mean/ urban influence mean)', n = 8($2^a/2^b$)) and continental (as 'mean (day mean/ night mean)', n = 22(11/11)) sites, together with temperature and supporting aerosol parameters (PM_{10} and carbonaceous mass fractions). LOQ = limit of quantification, nd = no data.

	Marine			Continental		
	c_{tot} (pg m^{-3})	Θ	MMD (µm)	c_{tot} (pg m^{-3})	Θ	MMD (µm)
FLT	226 (161/259)	0.07 (0.03/0.07)	0.58 (0.43/0.52)	342 (432/251)	0.11 (0.11/0.12)	0.062 (0.101/0.034)
PYR	158 (103/188)	0.04 (0.01/0.05)	0.21 (0.022/0.22)	226 (276/176)	0.18 (0.18/0.19)	0.075 (0.105/0.055)
BBN	4.1 (2.0/5.5)	0.01 (nd/0.05)	0.022 (nd/0.022)	15 (16/13)	0.61 (0.58/0.65)	0.079 (0.127/0.053)
BAA	2.8 (<LOQ/3.4)	0.28 (nd/0.29)	0.022 (nd/0.022)	16 (14/18)	0.91 (0.90/0.92)	0.070 (0.090/0.060)
TPH	12 (8.5/14)	0.02 (nd/0.05)	0.022 (nd/0.022)	23 (26/21)	0.51 (0.41/0.63)	0.070 (0.090/0.057)
CHR	23 (10/29)	0.22 (0.09/0.20)	0.15 (0.022/0.15)	41 (44/38)	0.75 (0.71/0.80)	0.074 (0.105/0.055)
Σ_6 4rPAH	426 (284/499)	0.07 (0.02/0.07)	0.31 (0.19/0.28)	663 (808/517)	0.21 (0.19/0.25)	0.071 (0.10/0.051)
3NACE	0.21 (0.17/0.39)	0.05 (0.00/0.14)	0.022 (nd/0.022)	1.0(1.0/1.0)	0.05 (0.01/0.11)	0.022 (nd/0.022)
5NACE	1.8 (1.5/2.0)	0.07 (0.00/0.00)	0.022 (nd/nd)	6.8 (7.6/6.0)	0.03 (0.01/0.05)	0.022 (0.022/0.022)
2NFLN	0.01 (<LOQ/0.15)	0.02 (nd/0.00)	1.19 (nd/nd)	0.035 (0.035/0.034)	0.00 (0.00/0.00)	nd
9NPHE	0.73 (0.84/0.55)	0.00 (0.00/0.00)	nd	0.21 (0.28/0.13)	0.36 (0.43/0.20)	0.022 (0.022/nd)

3NPHE	4.8 (3.4/5.0)	0.00 (nd/nd)	nd	7.4 (10.0/4.8)	0.24 (0.15/0.44)	0.109 (0.067/0.116)
9NANT	4.2 (1.1/8.2)	0.00 (0.00/0.00)	nd	22 (22/22)	0.23 (0.14/0.33)	0.022 (0.022/0.022)
2NFLT [c]	8.6 (3.8/11)	0.32 (nd/0.45)	0.040 (nd/0.080)	15 (13/18)	0.78 (0.54/0.95)	0.054 (0.035/0.050)
1NPYR	0.75 (0.21/1.4)	0.33 (0.00/0.58)	0.061 (nd/0.14)	1.1 (1.1/1.2)	0.82 (0.76/0.88)	0.030 (0.031/0.029)
2NPYR	2.5 (0.92/3.3)	0.53 (0.19/0.69)	0.058 (0.060/0.055)	1.3 (0.73/2.0)	0.93 (0.83/0.97)	0.070 (0.040/0.061)
7NBAA	<LOQ	nd	nd	2.5 (0.77/4.2)	0.91 (0.56/0.97)	0.074 (0.038/0.057)
6NCHR	0.02 (<LOQ/0.07)	1.00 (nd/1.00)	2.12 (nd/2.12)	0.01 (<LOQ/0.02)	1.00 (nd/1.00)	0.022 (nd/0.022)
Σ_{11}3-4rNPAH	23.7 (11.8/32.0)	0.22 (0.01/0.22)	0.34(0.33/0.34)	58 (56/59)	0.16 (0.13/0.17)	0.039 (0.036/0.040)
PM_{10} (µg/m³)	34.9 (21.0/55.5)		0.58 (1.13/0.62)	22.1 (19.5/24.5)		nd
EC (µg/m³)	0.11 (0.09/0.17)		0.03(0.05/0.03)	0.31 (0.28/0.33)		0.21(0.19/0.22)
OC (µg/m³)	1.9 (1.5/3.0)		0.17(0.16/0.15)	3.6 (3.3/3.9)		0.16(0.13/0.18)
T (°C)	25.6 (27.0/22.2)			23.1 (28.8/17.5)		

[a] 2 filter and 4 PUF samples i.e., No. 9, 10, 19 and 22 in Fig. S3
[b] 1 filter and 1 PUF sample i.e., No. 1 and 2 in Fig. S3
[c] co-eluted with 3NFLT, assuming $c_{3NFLT} = 0$